

Peterson Olefination: Unexpected Rearrangement in the Overcrowded Polycyclic Aromatic Ene Series

Naela Assadi,^[a] Sergey Pogodin,^[a] and Israel Agranat*^[a]

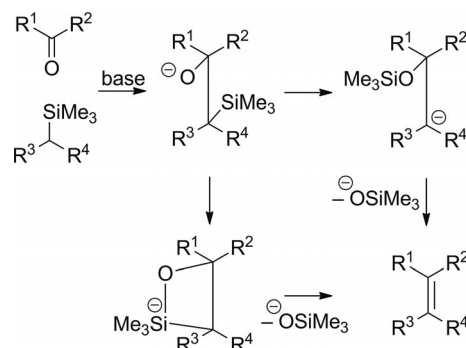
Keywords: Reaction mechanisms / Rearrangement / Olefination / Polycycles / Arenes / Density functional calculations

An attempted synthesis of the angularly annelated 9-(11'-benzo[*a*]fluoren-11'-ylidene)-9*H*-fluorene (**3**) through a Peterson olefination reaction between (9*H*-fluoren-9-yl)trimethylsilyl anion (**5a**) and 11*H*-benzo[*a*]fluoren-11-one (**6**) led to the linearly annelated 9-(11'-benzo[*b*]fluoren-11'-ylidene)-9*H*-fluorene (**4**), due to an unexpected rearrangement. The proposed mechanism of the rearrangement is illustrated. The core of the mechanism is an intramolecular Haller–Bauer cleavage of the naphthyl C^{11a'}–C^{11'} bond in the β-oxysilane

anion **11** (formed from **5a** and **6**) to give the 1-naphthyl anion (*E*)-**12**, followed by *E/Z* isomerization to (*Z*)-**12** and by proton migration to give the 3-naphthyl anion (*Z*)-**14**. The intramolecular nucleophilic addition of the naphthyl anion at C-3' of (*Z*)-**14** to the carbonyl carbon gives the β-oxysilane anion **15**, a benzo[*b*]fluorenylidene derivative. The mechanism is supported by the results of DFT calculations. The synthesis of **3** was achieved by application of Barton's double extrusion diazo–thione coupling method.

Introduction

The Peterson olefination reaction^[1–5] (Scheme 1) is a two-step synthesis of alkenes involving the addition of α-silyl carbanions to carbonyl groups to form β-hydroxysilyl intermediates, followed by the elimination of silols to form alkenes. The reaction is considered to be the silicon variation of the wide class of the Wittig-type reactions, involving additions of α-heteroatom-stabilized carbanions to aldehydes and ketones.^[4] The initial condensations are not stereoselective and the β-hydroxysilyl intermediates are formed as roughly 1:1 mixtures of *erythro* and *threo* isomers.^[3] The product stereochemistries are remarkably insensitive to the effects of counterion, solvent, added salts, variation of the carbanion-forming base, and temperature.^[6,7] However, the β-hydroxysilyl intermediates undergo *anti* elimination under acidic conditions and *syn* elimination under basic conditions, so both *E* and *Z* isomers can be obtained from a single β-hydroxysilyl diastereomer.^[8,9] The final eliminations might proceed either in a stepwise manner^[10,11] or by a concerted mechanism through the formation of oxasiletanide^[12] intermediates, although there appears to be overwhelming evidence in support of a stepwise mechanism.^[4]



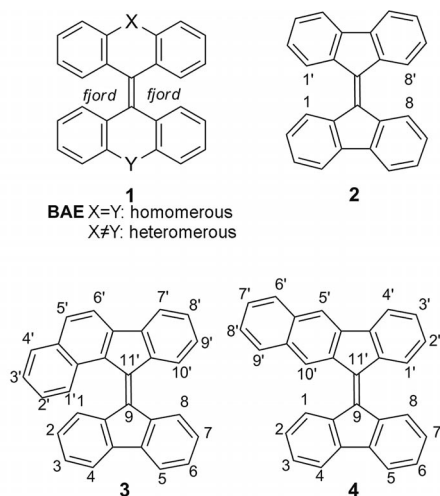
Scheme 1. Peterson olefination reaction.

Peterson olefination reactions have been extensively applied by Mills et al. in the synthesis of overcrowded bistricyclic aromatic enes (BAEs, **1**), including heteromeric bifluorenylidene (**1**, X ≠ Y) and diphenylmethylidene fluorenes.^[13–15] The 3,6-dimethyl derivative of the parent bifluorenylidene **2**, for example, was synthesized by addition of trimethylsilyl carbanion to 9*H*-fluorene to give (9*H*-fluoren-9-yl)trimethylsilane, which upon treatment with *n*BuLi and 3,6-methyl-9*H*-fluoren-9-one gave 3,6-dimethylbifluorenylidene.^[15]

In the course of our studies of overcrowded bistricyclic aromatic enes (BAEs),^[16,17] we have recently directed our attention to naphthologous analogues of BAEs.^[18] We attempted the synthesis of 9-(11'-benzo[*a*]fluoren-11'-ylidene)-9*H*-fluorene (**3**) by application of a Peterson olefination. Here, though, we report an unexpected rearrangement in the course of a Peterson olefination, in which instead of the target – the angularly annelated **3** – its consti-

[a] Organic Chemistry, Institute of Chemistry, The Hebrew University of Jerusalem, Philadelphia Bldg. #201/205, Edmond J. Safra Campus, Jerusalem 91904, Israel
E-mail: isria@vms.huji.ac.il

Supporting information for this article is available on the WWW under <http://dx.doi.org/10.1002/ejoc.201100789>.

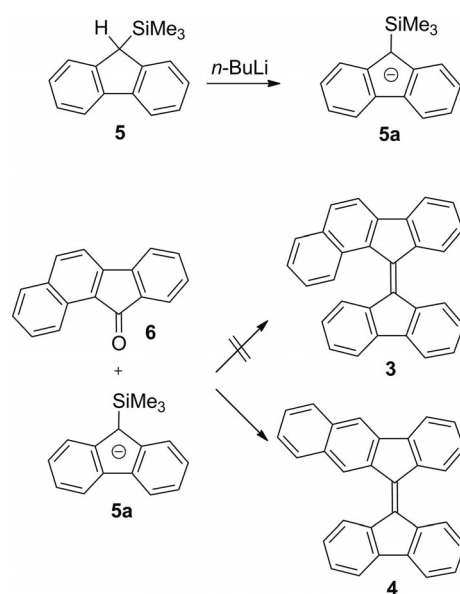


tutional isomer, the linearly annelated 9-(11'-benzo[*b*]fluoren-11'-ylidene)-9*H*-fluorene (**4**), was formed. The synthesis of **3** was eventually achieved by application of Barton's double extrusion diazo–thione coupling method,^[19–21] also known as the Barton–Kellogg olefination.^[21]

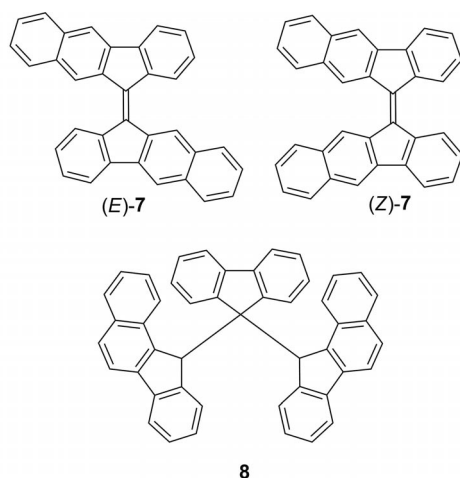
Results and Discussion

The attempted synthesis of **3** and the formation of the rearrangement product **4** are shown in Scheme 2. Treatment of a THF solution of (9*H*-fluoren-9-yl)trimethylsilane (**5**)^[22] with *n*BuLi gave the corresponding deep yellow carbanion **5a**. Addition of 11*H*-benzo[*a*]fluoren-11-one (**6**)^[23,24] at $-78\text{ }^{\circ}\text{C}$ and subsequent running of the reaction at room temperature for 14 hours gave a crude mixture of products after workup. Purification by column chromatography on silica gel gave the linearly annelated rearranged product **4**, identical to an authentic sample,^[25] as a red powder (m.p. $173\text{--}175\text{ }^{\circ}\text{C}$) in 4.5% yield. The structure of **4** was verified by ^1H NMR and ^{13}C NMR spectroscopy (vide infra). Compounds **2**^[26] (12% yield), **5** (45%), and **6** (4%) were also identified and characterized among the reaction products. There was no indication of the formation of the expected product **3**, neither in the crude product mixture, nor in the eluted chromatography fractions, as concluded from the absence of any ^1H NMR signal due to 2-H (vide infra) at $\delta = 6.87$ ppm. Likewise, (*E*)- and (*Z*)-11-(11'*H*-benzo[*b*]fluoren-11'-ylidene)-11*H*-benzo[*b*]fluorene [(*E*)-**7** and (*Z*)-**7**, below]^[25,27] were not formed, as was concluded from the absence of the ^1H NMR signals of their *fjord* region^[17] singlets [$\delta(10\text{-H}) = 8.90$ for (*E*)-**7** and 9.11 ppm for (*Z*)-**7**]. The mass spectrum of the crude reaction product showed a signal at $m/z = 592$, which could be assigned to a $\text{C}_{47}\text{H}_{28}$ species formed from two benzo[*a*]fluorenyl ($\text{C}_{17}\text{H}_{11}$) units and one fluorenylidene (C_{13}H_8) units, possibly derived from 9,9-bis(11*H*-benzo[*a*]fluorenyl)-9*H*-fluorene (**8**); it was not further characterized.

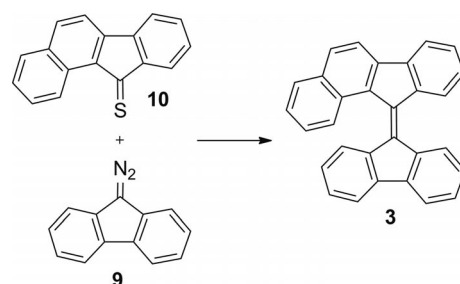
The angularly annelated **3** was eventually synthesized from 9-diazo-9*H*-fluorene (**9**) and 11*H*-benzo[*a*]fluoren-11-thione (**10**) by Barton's double extrusion diazo–thione coupling method (Scheme 3).^[19–21] The crude prod-



Scheme 2. Attempted synthesis of the BAE **3** and formation of the polycyclic aromatic ene (PAE) **4**.



uct from the coupling reaction between **10** and **9** was purified by column chromatography on silica gel to give **3** as a red powder (9% yield, m.p. $155\text{--}160\text{ }^{\circ}\text{C}$). The mass spectrum of **3** showed a signal at $m/z = 378$ [$\text{M}]^+$. The structure of **3** was established by ^1H NMR and ^{13}C NMR spectroscopy (vide infra).



Scheme 3. Synthesis of the PAE **3**.

NMR Spectroscopy

The ^1H NMR chemical shifts of **3** and **4** are depicted in Figure 1. The ^1H NMR spectrum of **2** is characterized by a low-field chemical shift of the *ffjord* region protons 1-H, 8-H, 1'-H, and 8'-H ($\delta = 8.39$ ppm), which is characteristic of a twisted conformation in BAEs.^[25] The ^1H NMR chemical shifts of the *ffjord* region protons of **2–4**, (*E*)-**7**, and (*Z*)-**7** are all given in Table 1. In **4** the corresponding protons appear at 8.54 (8-H), 8.36 (1-H), 8.40 (1'-H), and 8.85 ppm (10'-H), indicating a twisted conformation.^[25] A 2D-NOESY experiment indicated NOE interactions between 1-H and 10'-H and between 8-H and 1'-H. The ^1H NMR spectrum of **3** differs from that of **4**. The *ffjord* region protons 8-H and 10'-H appear, as expected, at $\delta = 8.41$ and 8.44 ppm, respectively, similarly to the corresponding protons 1-H and 1'-H of **4** and 1'-H, 8-H of **2**. However, the other two *ffjord* region protons of **3** appear at $\delta = 7.20$ (1-H) and 7.99 ppm (1'-H), unlike the corresponding protons 8-H and 10'-H of **4**. The different effects of the angular benzo[*a*]annulation in **3** versus the linear benzo[*b*]annulation of **4** on the *ffjord* region protons are noted.

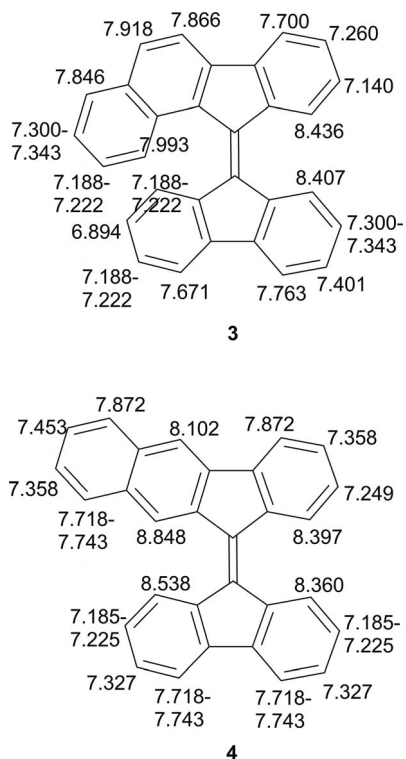


Figure 1. ^1H NMR chemical shifts of the PAEs **3** and **4**.

In **4**, the naphthalene *ffjord* region proton 10'-H is shifted downfield (relative to 1-H, 8-H, and 1'-H) to $\delta = 8.85$ ppm [similarly to 10-H in (*E*)-**7**, $\delta = 8.90$ ppm^[26]]. In **3**, the naphthalene *ffjord* region 1'-H is shifted upfield [$\delta(1'-\text{H}) = 7.99$ ppm] relative to $\delta(8-\text{H})$ and $\delta(10'-\text{H})$. Interestingly, the *ffjord* region 1-H of **3** facing the naphthalene ring is shifted considerably upfield [$\delta(1-\text{H}) = 7.20$ ppm]. More strikingly, the signal due to 2-H of **3** appears at $\delta = 6.89$ ppm as com-

Table 1. Experimentally measured and calculated ^1H and ^{13}C chemical shifts for the PAEs **2–4** and **7**.

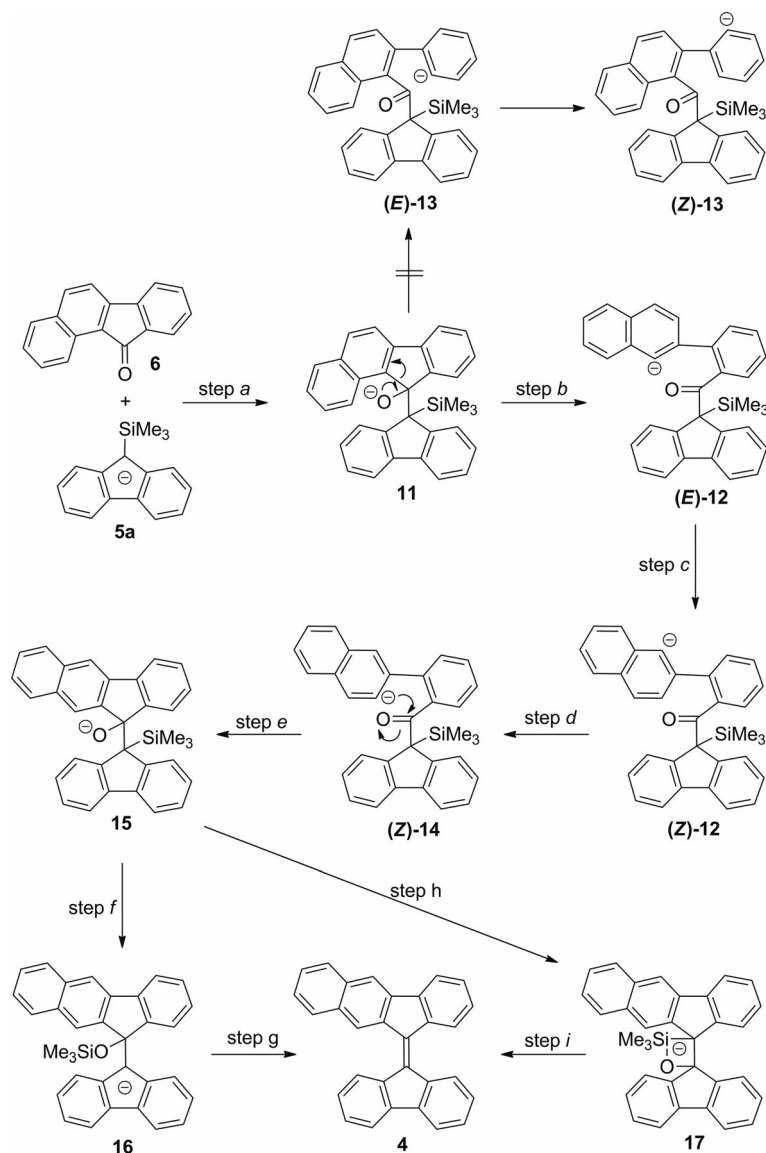
	2 ^[a]	3 ^[a]	3 ^[b]	4 ^[a]	4 ^[b]	(<i>E</i>)- 7 ^[a]	(<i>Z</i>)- 7 ^[a]
1'-H		7.993	8.13	8.397	9.05		
2'-H		7.188–7.222	7.35	7.249	7.84		
3'-H		7.300–7.343	7.43	7.358	7.54		
4'-H		7.846	7.92	7.872	7.61		
5'-H		7.918	7.97	8.102	7.99		
6'-H		7.866	7.97	7.872	8.19		
7'-H		7.700	7.78	7.453	8.01		
8'-H		7.260	7.32	7.358	7.47		
9'-H		7.140	7.18	7.718–7.743	7.31		
10'-H		8.436	8.56	8.848	8.61		
1-H	8.39	7.188–7.222	7.30	8.360	8.73	8.64	8.46
2-H	7.23	6.894	6.90	7.185–7.225	7.27		
3-H	7.35	7.188–7.222	7.27	7.327	7.43		
4-H	7.72	7.671	7.76	7.718–7.743	7.86		
5-H	7.72	7.763	7.86	7.718–7.743	7.84		
6-H	7.35	7.401	7.45	7.327	7.41		
7-H	7.23	7.300–7.343	7.35	7.185–7.225	7.26		
8-H	8.39	8.407	8.51	8.538	8.53		
10-H						8.90	9.11

[a] Experimentally measured (500 MHz, CHCl_3) chemical shifts. [b] Calculated (GIAO) chemical shifts at B3LYP/6-311G(d,p) geometry.

pared with 7.23 and 7.20 ppm in **2** and **4**, respectively. The pronounced upfield shifts of 2-H and 1-H in **3** are probably due to shielding by the diamagnetic ring current of the opposite naphthalene ring.^[28] In a strong magnetic field, nuclei located over an aromatic ring experience a diminished magnetic field as a result of the induced magnetic field caused by the circulating π electrons.^[28] This shielding effect indicates that in solution, 1-H and 2-H of **3**, in contrast to the corresponding 1-H and 2-H of **4**, are positioned somewhat above the plane of the naphthalene ring, which is consistent with the results of the DFT calculations (vide infra).

Mechanism of Rearrangement

Scheme 4 depicts a proposed mechanism of the rearrangement accompanying the Peterson olefination reaction between **5a** and **6** leading to **4**. Nucleophilic addition of the trimethylsilyl carbanion **5a** to the ketone **6** (step a) gives the β -oxysilane anion **11**. The crucial step of the proposed mechanism is an intramolecular Haller–Bauer cleavage (a base-induced cleavage of a carbon–carbon bond in a non-enolizable ketone)^[29,30] of the $\text{C}^{11a'}\text{–C}^{11'}$ bond of **11** to form the 1-naphthyl anion (*E*)-**12** (step b). The Haller–Bauer reaction would be expected to cleave the 1-naphthyl $\text{C}^{11a'}\text{–C}^{11'}$ bond of **11** to give the 1-naphthyl anion (*E*)-**12** in preference to the phenyl $\text{C}^{10a'}\text{–C}^{11'}$ bond to give the



Scheme 4. Proposed mechanism of the Peterson olefination and rearrangement leading to **4**.

phenyl anion **(E)-13**, because the resulting 1-naphthyl anion **(E)-12** would be expected to be more stable than the alternative phenyl anion **(E)-13**.^[24,31,32]

The **(E)-12** diastereomer then undergoes *E/Z* isomerization to give the more stable (vide infra) **(Z)-12** diastereomer (step c). The *E* and *Z* stereodescriptors in **12** refer to the conformations in which the carbonyl group and the anionic carbon are *cis* and *trans* (to each other), respectively. The rearrangement occurs when the 1-naphthyl anion **(Z)-12** isomerizes to its constitutional isomer, the 3-naphthyl anion **(Z)-14**, by proton migration (step d). The anion **(Z)-14** is well positioned for the following step: the intramolecular nucleophilic addition of the naphthyl anion at C-3' of **(Z)-14** to the carbonyl carbon to give the β -oxysilane anion **15**, a constitutional isomer of **11** (step e). The anion **15** then undergoes a migration of the trimethylsilyl group to the oxygen atom at C-11' to give the carbanion **16** (step f). This step is essentially the Brook rearrangement (i.e., a base-

catalyzed intramolecular migration of a silyl group from a carbon atom to an oxygen atom by a mechanism involving a hypervalent pentacoordinate silicon species).^[33,34] Elimination of the silanol group from **16** and the formation of the $C^{11'}=C^9$ double bond yields the final product: the PAE **4** (step g). Alternatively, the elimination of the silanol group from **15** could proceed through the formation of the four-membered oxasiletanide intermediate **17** (step h), which could lose the silanol group to give **4** (step i). Step f and step g are consistent with the reported mechanism of the Peterson olefination reaction.^[4] The proposed mechanism of the rearrangement accompanying the Peterson olefination of **6** leading to **4** is in agreement with the results of the DFT study (vide infra).

DFT Study

DFT methods are capable of generating a variety of isolated molecular properties quite accurately, especially with

the aid of the hybrid functional, and in a cost-effective way.^[35,36] The B3LYP hybrid functional has been successfully employed to treat BAEs^[37,38] and overcrowded naphtho analogues of mono-bridged tetraarylethylenes.^[18] The PAEs **3** and **4**, the siloxane anions **18** and **16**, the β -hydroxysilanes **19** and **20** (the *O*-protonated derivatives of the β -oxysilanes **11** and **15**, respectively), the lithium salts **21** and **22** of **11** and **15**, respectively, the 1-naphthyl anion (*Z*)-**12**, the 3-naphthyl anion (*Z*)-**14**, the phenyl anion (*Z*)-**13**, and the parent 1-naphthalenyl anion **23** and 2-naphthalenyl anion **24** were subjected to a computational DFT study of their conformations. The B3LYP/6-311G(d,p) relative Gibbs free energies (ΔG_{298}) of these species are presented in Table 2. Table 3 gives selected geometrical parameters of these species: the torsion angles (τ_1 and τ_2) around the central $C^{11'}-C^9$ bond at the *ffjord* region, the torsion angle (ζ) $O-C^{11'}-C^9-Si$, describing the rotational conformers around $C^{11'}-C^9$ single bond, the dihedral angles between the benzene and the naphthalene rings of the benzo-fluorenyl moiety (v_1), between the benzene rings of the fluorenyl moiety (v_2), and between the benzofluorenyl and fluorenyl moieties (v_3), and the pyramidalization angles (χ) at C-11', C-9, C-11a', C-10a', C-9a, and C-8a. In addition, Table S1 in the Supporting Information shows the shortest contact distances in the compounds under study.

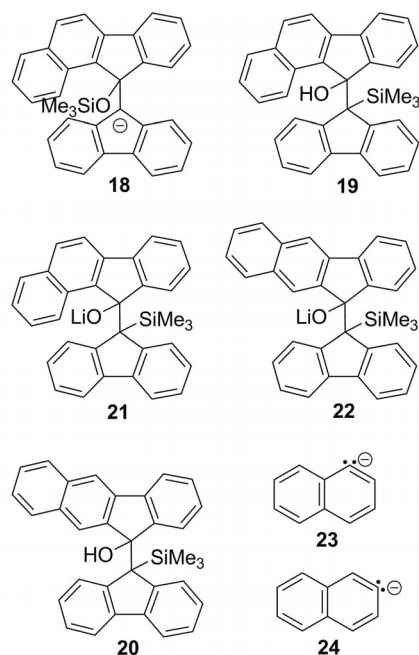


Figure 2 depicts the DFT calculated structures of **3** and **4**. The benzo[*b*]fluorenylidene PAE **4** was found to be 22.5 kJ mol⁻¹ more stable than the benzo[*a*]fluorenylidene PAE **3**. Likewise, the β -hydroxysilane *sc*-**20**, its lithium salt *sc*-**22**, and the siloxane *sc*-**16** were more stable than their constitutional isomers *sc*-**19**, *sc*-**21**, and *sc*-**18** by 27.9, 24.9, and 5.8 kJ mol⁻¹, respectively. The benzo[*b*]fluorenylidene derivatives **4**, *sc*-**20**, and *sc*-**22** are less overcrowded than the corresponding benzo[*a*]fluorenylidene derivatives **3**, *sc*-**19**,

Table 2. Relative free energies (ΔG_{298} , kJ mol⁻¹) of the PAEs **3** and **4** and related species.

		[a]	B3LYP/6-311G(d,p)	B3LYP/6-311+G(d,p)
3	<i>t</i>	C_1	22.45	
4	<i>t</i>	C_1	0.00	
12	<i>Z</i>	C_1	0.00	0.00 ^[b]
13	<i>Z</i>	C_1	23.54	
14	<i>Z</i>	C_1	11.06	9.57 ^[b]
18	<i>sc</i>	C_1	-269.78	
16	<i>sc</i>	C_1	-275.55	
19	<i>sc</i>	C_1	27.91	
19	<i>ac</i>	C_1	57.98	
20	<i>sc</i>	C_1	0.00	
20	<i>ac</i>	C_1	30.18	
21	<i>sc</i>	C_1	24.85	
22	<i>sc</i>	C_1	0.00	
23	-	C_s	0.00	0.00
24	-	C_s	6.69	5.49

[a] *t*: twisted conformation; *sc*: synclinal conformation; *ac*: anti-clinal conformation. [b] Single-point energy calculation on the B3LYP/6-311G(d,p) geometry.

Table 3. Selected dihedral and torsion angles in the PAEs **3** and **4** and in related species.

[a]		τ_1	τ_2	ζ	χ	χ	χ	v_1	v_2	v_3
					C-11'	C-11a'	C-10a'			
		[°]	[°]	[°]	[°]	[°]	[°]	[°]	[°]	[°]
3	<i>t</i>	-34.5	-	-10.6	11.1	-11.4	6.1	3.4	51.1	
		-39.7	-	-5.5	9.7	-10.5				
4	<i>t</i>	-34.1	-	0.2	10.3	-10.1	1.7	2.7	43.0	
		-34.2	-	-0.1	10.7	-10.5				
2	<i>t</i>	-33.9	-	0.0	-10.6	-	2.6	2.6	42.5	
12	<i>Z</i>	-87.5	-29.6	4.8	10.2	-	34.6	6.0	-	
				60.5	-0.1	-2.1				
14	<i>Z</i>	-86.8	-29.5	-5.3	-9.9	-	43.2	6.1	-	
				-60.9	-0.1	2.2				
19	<i>sc</i>	-58.6	-58.1	-67.9	5.5	0.2	17.7	1.4	46.4	
		-59.0		67.5	-3.0	-2.4				
20	<i>sc</i>	-62.7	-60.4	65.9	-1.2	5.3	12.4	0.4	58.2	
		-61.9		-66.9	2.3	1.9				
21	<i>sc</i>	-59.3	-60.7	-72.3	7.7	3.6	18.4	0.9	44.9	
		-64.1		67.5	-1.9	-1.5				
22	<i>sc</i>	-66.2	-63.1	70.0	-6.4	-8.0	12.2	0.7	58.1	
		-63.1		-67.0	1.5	0.8				
18	<i>sc</i>	50.7		-65.6	1.2	-1.2	0.5	1.0	83.9	
		114.9		1.3	0.6	0.4				
16	<i>sc</i>	23.8		64.3	-1.5	0.5	2.2	4.0	68.9	
		81.2		-6.9	-2.6	-0.1				

[a] *t*: twisted conformation; *sc*: synclinal conformation; *ac*: anti-clinal conformation.

and *sc*-**21**. Indeed, a comparison of the geometries of **3** and **4** shows that the *ffjord* torsion angle τ_2 ($C^{11a'}-C^{11'}-C^9-C^{9a}$) of **3** is 5.5° greater than the corresponding τ_2 of **4**. Moreover, the dihedral angles v_1 and v_3 of **3** are 4.4° and 8.1° greater than the corresponding angles of **4**. Most striking are the pronounced pyramidalization angles of the carbon atoms of the central $C^{11'}=C^9$ double bond of **3** – $\chi(C-11') = -10.6^\circ$ and $\chi(C-9) = -5.5^\circ$ – whereas the corresponding angles in **4** are negligible (0.2° and -0.1°). The *syn* pyramidalization of the $C^{11'}=C^9$ bond in **3** is notable. The

large dihedral angles (ν_3) and pyramidalization (χ) values in **19–22** are expected, due to the sp^3 hybridization of C-9 and C-11', and do not reflect the degree of overcrowding. However, the dihedral angles (ν_1) in *sc-19* and *sc-21*, describing the loss of conjugation between phenyl and naphthyl aromatic systems, are larger than the corresponding dihedral angles in *sc-20* and *sc-22* (by 5.3° and 6.2°), showing the greater steric strain in the former species. The nonbonding C...H distances in **4**, *sc-20*, and *sc-22* are also somewhat larger than the corresponding distances in **3**, *sc-19*, and *sc-21* (Table S1 in the Supporting Information). The siloxanes *sc-16* and *sc-18* are not overcrowded, due to very large dihedral angles (ν_3). It is known that upon oxidation or reduction of the parent BAE **2** the twist angle between its two bistricyclic ring systems increases, reaching 58° in **2**²⁻ and 64° in **2**²⁺, in comparison with 33.9° in **2**.^[39,40]

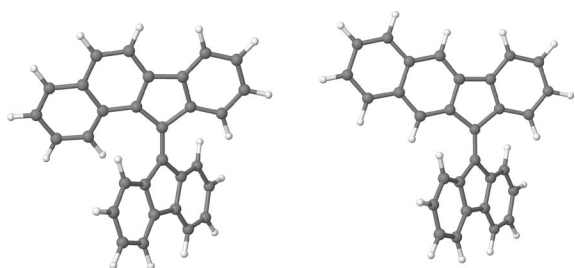


Figure 2. Calculated structures of **3** and **4** at B3LYP/6-311G(d,p).

It is noteworthy that according to the proposed mechanism of the rearrangement, the 1-naphthyl anion (*Z*)-**12** rearranges to the 3-naphthyl anion (*Z*)-**14** even though (*Z*)-**12** is 11.1 kJ mol^{-1} more stable than (*Z*)-**14**. The (*Z*)-**12**→(*Z*)-**14** rearrangement (step d) is probably not the rate-determining step of the reaction leading to **4**. The course of the reaction is dictated by the relative stabilizations of the benzo[*b*]fluorenylidene constitutional isomers (**4** vs. **3** by 22.5 kJ mol^{-1} , **20** vs. **19** by 27.9 kJ mol^{-1} , and **16** vs. **18** by 5.8 kJ mol^{-1}). Single-point calculations of (*Z*)-**12** and (*Z*)-**14** with diffuse functions on the heavy atoms [at B3LYP/6-311+(d,p)//B3LYP/6-311(d,p)] indicated a similar trend, with $\Delta E_{\text{Tot}} = 9.6 \text{ kJ mol}^{-1}$, relative to $\Delta E_{\text{Tot}} = 13.7 \text{ kJ mol}^{-1}$ at B3LYP/6-311G(d,p). At these levels, the 1-naphthalenyl anion **23** is more stable than the 2-naphthalenyl anion **24**: $\Delta G_{298} = 6.7 \text{ kJ mol}^{-1}$ [B3LYP/6-311G(d,p)] and 5.5 kJ mol^{-1} [B3LYP/6-311+G(d,p)]. The literature B3LYP/DZP++ZPVE-corrected energy of **24** relative to **23** is 5.3 kJ mol^{-1} . This difference is attributed both to steric effects of repulsion between the lone electron pair and the adjacent hydrogen atoms and to the hybridization effects of the reduction in the bond angle at the anionic center.^[32] NBO calculations for the 1-naphthyl anion (*Z*)-**12** and the 3-naphthyl anion (*Z*)-**14** indicate that most of the negative charge is concentrated on the naphthyl moieties: -0.824 [(*Z*)-**12**] and -0.855 [(*Z*)-**14**]. As might be expected, in (*Z*)-**12** a substantial part of the charge is located at C-1 (-0.313), whereas in (*Z*)-**14** a substantial part of the charge is located at C-3 (-0.351). These values are higher than the corresponding charges at C-1 of **23** (-0.261) and at C-2 of **24** (-0.244). This renders

the steric effect of electron–electron repulsion even more pronounced, which is reflected in greater stabilization of (*Z*)-**12** than of (*Z*)-**14**. Note that the HOMA aromaticity indices^[41] calculated for the five- and six-membered rings of (*Z*)-**12**, (*Z*)-**14**, **19**, **20**, **3**, and **4** did not indicate any significant differences between the benzo[*a*]fluorenylidene and benzo[*b*]fluorenylidene series. The dihedral angles between the phenyl and the naphthalene planes in (*Z*)-**12** and (*Z*)-**14** are 34.6° and 43.2° , respectively, indicating more effective conjugation between the aromatic moieties in (*Z*)-**12** than in (*Z*)-**14**.

The stereochemistry of the β -hydroxysilanes **19** and **20** deserves a comment. In each case, two conformers were located with the following ζ torsion angles: -58.1° in *synclinal* **19** (*sc-19*), 132.8° in *anticlinal* **19** (*ac-19*) (see Figure 3), and -60.4° in *sc-20* and 177.1° in *antiperiplanar* **20** (*ap-20*) (see Figure 4). The conformer *sc-19* was more stable than *ac-19* by 24.5 kJ mol^{-1} ; *sc-20* was more stable than *ap-20* by 31.3 kJ mol^{-1} . In the *synclinal* conformers, the oxygen and silicon atoms are well positioned for intramolecular cyclization to the four-membered oxasiletanides such as **17**.

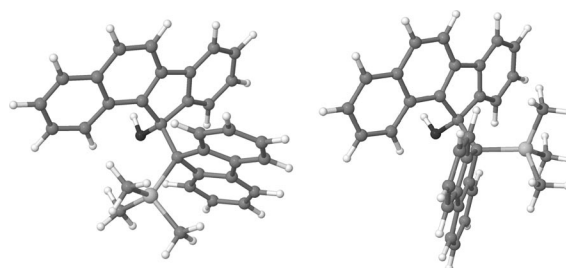


Figure 3. Calculated structures of *sc-19* and *ac-19* at B3LYP/6-311G(d,p).

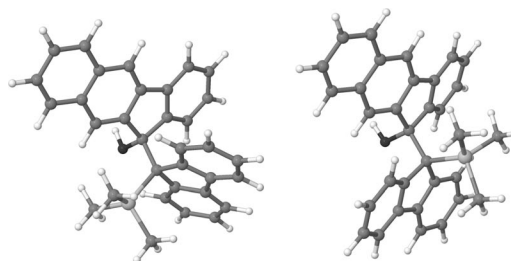


Figure 4. Calculated structures of *sc-20* and *ap-20* at B3LYP/6-311G(d,p).

Conclusions

The synthesis of the PAE **3** can be achieved by applying the Barton diazo–thione coupling method to diazofluorene (**9**) and benzo[*a*]fluorene-*thione* (**10**). In contrast, the Peterson olefination reaction between the fluorene derivative **5a** and benzo[*a*]fluorenone (**6**) leads to the PAE **4**, a constitutional isomer of **3**. This rearrangement sheds new light on the mechanism of Peterson olefination in the series of polycyclic aromatic ketones.

Experimental Section

Melting points are uncorrected. All NMR spectra were recorded with a Bruker DRX 500 spectrometer. ^1H NMR spectra were recorded at 500.2 MHz with CDCl_3 as solvent and as internal standard [$\delta(\text{CHCl}_3) = 7.26$ ppm]. ^{13}C NMR spectra were recorded at 125.78 MHz with CDCl_3 as solvent and as internal standard [$\delta(\text{CDCl}_3) = 77.0$ ppm]. Complete assignments were made through two-dimensional correlation spectroscopy (DQF-COSY, HSQC, NOESY and HMBC). Mass spectrometry was performed with a Voyager-DETM PRO workstation and the matrix-assisted laser desorption/ionization (MALDI) technique (2,5-dihydroxybenzoic acid matrix). Petroleum ether (PE, b.p. 40–60 °C), THF, and benzene were dried on sodium and freshly distilled.

9H-Fluoren-9-yltrimethylsilane (5): Compound **5** was prepared by a literature procedure with some modifications.^[13] Fluorene (0.5 g, 3.0 mmol) was dissolved in dry THF (20 mL) in a round-bottomed flask containing a magnetic stirrer and fitted with a septum. The reaction mixture was cooled to -78 °C under argon. *n*BuLi (2.4 mL, 3.9 mmol, 1.6 M in hexane) was added. The color of the reaction mixture turned orange. After 0.5 h, the reaction mixture was allowed to warm to 0 °C and stirred for an additional 10 min. The reaction mixture was cooled again to -78 °C and trimethylsilyl chloride (0.8 mL, 6.02 mmol) was added; the color turned yellow. The reaction mixture was stirred for 0.5 h and then allowed to warm to 0 °C and stirred for 2 h. It was quenched with saturated aqueous NH_4Cl and extracted with CH_2Cl_2 , the organic fraction was dried on MgSO_4 and filtered, and the solvent was evaporated under reduced pressure. Trituration of the crude product with PE gave **5** as a yellow powder, 0.58 g, yield 81%, m.p. 100 °C (ref.^[22] 97.5–99.5 °C). ^1H NMR (CDCl_3): $\delta = -0.063$ [s, 9 H, Si(CH_3)], 3.868 (s, 1 H, 9-H), 7.295 (td, $^3J = 7.5$, $^4J = 1.0$ Hz, 2 H, 2-H, 7-H), 7.346 (t, $^3J = 7.5$ Hz, 2 H, 3-H, 6-H), 7.506 (d, $^3J = 7.0$, $^4J = 1.0$ Hz, 2 H, 1-H, 8-H), 7.858 (d, $^3J = 7.5$ Hz, 2 H, 4-H, 5-H) ppm. ^{13}C NMR (CDCl_3): $\delta = -2.69$ [Si(CH_3)], 42.74 (C-9), 119.87 (C-4, C-5), 123.98 (C-1, C-8), 125.16 (C-3, C-7), 125.93 (C-2, C-6), 140.40 (C-4a, C-4b), 145.69 (C-8a, C-9a) ppm.

9-(11'-H-Benzo[b]fluoren-11'-ylidene)-9H-fluorene (4): In a round-bottomed flask containing a magnetic stirrer and fitted with a septum, **5** (0.46 g, 1.9 mmol) was dissolved in dry THF (30 mL). The reaction mixture was cooled to -78 °C under argon and *n*BuLi (1.5 mL, 2.5 mmol, 1.6 M in hexane) was added. The color of the reaction mixture turned deep yellow. After 0.5 h, the reaction mixture was allowed to warm to 0 °C and stirred for 10 min. The reaction mixture was then cooled again to -78 °C and a solution of the ketone **6**^[23,24] (0.5 g, 1.9 mmol) in THF (20 mL) was added dropwise. The color turned orange. After 0.5 h, the reaction mixture was allowed to warm to 0 °C and stirred overnight. The reaction mixture was quenched with saturated aqueous NH_4Cl , extracted with CH_2Cl_2 , dried on MgSO_4 , and filtered, and the solvent was evaporated under reduced pressure. The crude product was obtained as an orange powder (0.25 g). NMR spectroscopy of the crude product indicated the presence of the following compounds: **2**, **4**, **5**, and **6**. The crude product was purified by column chromatography on silica gel, with elution with PE/ CH_2Cl_2 (99:1). The following fractions were eluted:

9H-Fluoren-9-yltrimethylsilane (5): Yellow crystals, 0.21 g, yield 45%.

Bifluorenylidene (2): Red-orange crystals, m.p. 190 °C (ref.^[26] m.p. 191–198°), 0.079 g, yield 12%. ^1H NMR (CDCl_3): $\delta = 7.211$ (t, 2 H, 2-H, 9-H), 7.332 (t, 2 H, 3-H, 6-H), 7.709 (d, 2 H, 4-H, 5-H), 8.386 (d, 2 H, 1-H, 8-H) ppm. ^{13}C NMR (CDCl_3): $\delta = 119.89$ (C-

4, C-5), 126.73 (C-1, C-8), 126.85 (C-2, C-7), 129.15 (C-3, C-6), 138.28 (C-8a, C-9a), 141.01 (C-9, C-9'), 141.31 (C-4a, C-4b) ppm.

9-(11'-H-Benzo[b]fluoren-11'-ylidene)-9H-fluorene (4): Red powder 0.017 g, yield 4.5%, m.p. 173–175 °C (ref.^[25] 175–180 °C). ^1H NMR (CDCl_3): $\delta = 7.185$ – 7.225 (m, 2 H, 2-H, 7-H), 7.249 (td, $^3J = 7.5$, $^4J = 1.0$ Hz, 1 H, 2'-H), 7.327 (2 × td, $^3J = 7.5$, $^3J = 6.5$, $^4J = 1.0$ Hz, 2 H, 3-H, 6-H), 7.358 (2 × td, 2 H, 3'-H, 8'-H), 7.453 (td, $^3J = 7.4$, $^3J = 7.3$, $^4J = 1.5$, $^4J = 1.0$ Hz, 1 H, 7'-H), 7.718–7.743 (m, 3 H, 4-H, 5-H, 9'-H), 7.872 (ddd, $^3J = 7.0$, $^5J = 0.5$ Hz, 2 H, 4'-H, 6'-H), 8.102 (s, 1 H, 5'-H), 8.360 (d, $^3J = 8.0$ Hz, 1 H, 1-H), 8.397 (d, $^3J = 8.0$ Hz, 1 H, 1'-H), 8.538 (d, $^3J = 8.0$ Hz, 1 H, 8-H), 8.848 (s, 1 H, 10'-H) ppm. ^{13}C NMR (CDCl_3): $\delta = 117.96$ (C-5'), 119.89 (C-4), 119.96 (C-5), 120.60 (C-4'), 125.85 (C-8), 125.86 (C-8'), 126.26 (C-1), 126.52 (C-10'), 126.77 (C-1'), 126.78 (C-7), 126.90 (C-2), 126.98 (C-7'), 127.48 (C-2'), 128.36 (C-6'), 128.89 (C-3), 128.96 (C-6), 129.45 (C-9'), 129.48 (C-3'), 133.08 (C-9a'), 134.04 (C-5a'), 137.00 (C-10a'), 138.33 (C-9a), 138.55 (C-4b'), 138.65 (C-8a), 139.71 (C-9), 140.09 (C-11a'), 140.99 (C-11'), 141.14 (C-4a, C-4a'), 141.16 (C-4b) ppm. 2D NMR NOESY experimentation indicated NOE interaction between 1-H and 10'-H and likewise between 8-H and 1'-H.

11H-Benzo[a]fluoren-11-one (6): Orange powder, 0.020 g, yield 4%.

9-(11'-H-benzo[a]fluoren-11'-ylidene)-9H-fluorene (**3**) was not identified among the reaction products.

9-(11'-H-Benzo[a]fluoren-11'-ylidene)-9H-fluorene (3): The diazo compound **9**^[42] (0.08 g, 0.41 mmol) was added to a stirred solution of the thione **10** (0.10 g, 0.14 mmol, prepared analogously to 11H-benzo[b]fluorene-11-thione,^[25] from **6** and Lawesson's reagent) in boiling benzene (20 mL) protected by a CaCl_2 tube. The color of the reaction mixture was red. After having been heated at reflux for 12 h, the reaction mixture was allowed to cool to room temp., and the solvent was removed under reduced pressure. The crude product was purified by column chromatography on silica gel, eluted by PE. The desired product **3** was isolated and obtained as a red powder (0.058 g, yield 9%). M.p. 155–160 °C. ^1H NMR (CDCl_3): $\delta = 6.865$ (td, $^3J = 7.5$, $^4J = 1.0$ Hz, 1 H, 2-H), 7.148 (td, $^3J = 7.5$, $^4J = 1.5$ Hz, 1 H, 9'-H), 7.178 (dd, $^3J = 6.5$, $^4J = 1.5$ Hz, 1 H, 1-H), 7.194–7.231 (m, 2 H, 2'-H, 3-H), 7.272 (td, $^3J = 8.0$, $^3J = 7.5$ Hz, 1 H, 8'-H), 7.309–7.348 (m, 2 H, 3'-H, 7-H), 7.406 (td, $^3J = 7.5$, $^4J = 1.0$ Hz, 1 H, 6-H), 7.689 (d, $^3J = 7.5$ Hz, 1 H, 4-H), 7.718 (d, $^3J = 7.0$ Hz, 1 H, 7'-H), 7.778 (d, $^3J = 7.5$ Hz, 1 H, 5-H), 7.861 (d, $^3J = 8.0$ Hz, 1 H, 4'-H), 7.887 (d, $^3J = 8.0$ Hz, 1 H, 6'-H), 7.936 (d, $^3J = 8.0$ Hz, 1 H, 5'-H), 7.982 (d, $^3J = 8.5$ Hz, 1 H, 1'-H), 8.414 (d, $^3J = 7.5$ Hz, 1 H, 8-H), 8.442 (d, $^3J = 8.0$ Hz, 1 H, 10'-H) ppm. ^{13}C NMR (CDCl_3): $\delta = 118.47$ (C-6'), 119.62 (C-4), 119.74 (C-7'), 120.18 (C-5), 124.80 (C-10'), 124.93 (C-3'), 126.75 (C-2, C-7), 127.34 (C-2'), 127.44 (C-9'), 128.03 (C-1), 128.60 (C-8'), 128.78 (C-8), 128.83 (C-3), 129.00 (C-1'), 129.43 (C-4'), 129.50 (C-6), 129.95 (C-11b'), 131.76 (C-5'), 132.24 (C-11a'), 134.29 (C-4a'), 138.53 (C-8a), 139.56 (C-9a), 139.99 (C-10a'), 140.29 (C-6b'), 140.52 (C-11), 140.55 (C-4a), 142.30 (C-4b), 142.33 (C-6a'), 142.62 (C-9) ppm. Mass spectrometry showed a peak at $m/z = 378$ [M]⁺.

11H-Benzo[a]fluoren-11-one (6): Orange powder, 0.082 g, yield 18%, m.p. 129 °C (ref.^[24] 132 °C), also identified among the reaction products. ^1H NMR (CDCl_3): $\delta = 7.259$ (t, $^3J = 8.2$, $^3J = 6.4$ Hz, 1 H, 9-H), 7.405–7.478 (m, 3 H, 3-H, 7-H, 8-H), 7.586 (td, $^3J = 8.4$, $^4J = 1.0$, $^5J = 0.6$ Hz, 2 H, 2-H, 6-H), 7.623 (d, $^3J = 8.2$ Hz, 1 H, 10-H), 7.771 (d, $^3J = 8.3$ Hz, 1 H, 4-H), 7.971 (d, $^3J = 8.2$ Hz, 1 H, 5-H), 8.974 (d, $^3J = 8.5$ Hz, 1 H, 1-H) ppm. ^{13}C NMR (CDCl_3): $\delta = 118.02$ (C-6), 119.92 (C-7), 123.79 (C-10), 124.26 (C-1), 126.38 (C-8), 126.83 (C-11a), 128.49 (C-4), 129.22 (C-9), 129.40 (C-2), 130.15 (C-11b), 134.16 (C-3), 134.39 (C-4a),

134.55 (C-10a), 135.85 (C-5), 143.85 (C-6b), 146.11 (C-6a), 195.36 (C-11) ppm.

Computational Details: The quantum mechanical calculations were performed with the Gaussian03^[43] package. Becke's three-parameter hybrid density functional B3LYP^[44] with the non-local correlation functional of Lee, Yang, and Parr^[45] was used. The split valence 6-311G(d,p) basis set was employed. In the case of the naphthyl anion derivatives **12** and **14**, single-point B3LYP/6-311+G(d,p) calculations on the B3LYP/6-311G(d,p) geometry were carried out. The naphthalene anions **23** and **24** were fully optimized at the B3LYP/6-311+G(d,p) level. All structures were fully optimized. Symmetry constraints for **2** (D_2), **23**, and **24** (C_s) were used. Vibrational frequencies were calculated to verify the natures of the stationary points; all calculated structures were found to be minima. Non-scaled thermal corrections to Gibbs' free energy were used.

Supporting Information (see footnote on the first page of this article): ¹H and ¹³C NMR spectra of PAEs **3** and **4**, total and relative energies, selected shortest non-bonding distances, and calculated geometries of the species under study.

- [1] Z. Wang, *Peterson Olefination*, in: *Comprehensive Organic Name Reactions and Reagents*, Wiley, **2000**, vol. 2, chapter 491, pp. 2176–2181.
- [2] L. Birkofer, O. Stuhl, *Top. Curr. Chem.* **1980**, *88*, 33–88.
- [3] D. J. Ager, *Synthesis* **1984**, 384–398.
- [4] L. F. van Staden, D. Gravestock, D. J. Ager, *Chem. Soc. Rev.* **2002**, *31*, 195–200.
- [5] N. Kano, T. Kawashima, *The Peterson and Related Reactions*, in: *Modern Carbonyl Olefination* (Ed.: T. Takeda), Wiley-VCH, Weinheim, **2004**, chapter 2, pp. 18–103.
- [6] A. R. Bassindale, R. J. Ellis, P. G. Taylor, *Tetrahedron Lett.* **1984**, *25*, 2705–2708.
- [7] A. R. Bassindale, R. J. Ellis, J. C.-Y. Lau, P. G. Taylor, *J. Chem. Soc. Perkin Trans. 2* **1986**, 593–597.
- [8] P. F. Hudrlik, D. Peterson, R. J. Rona, *J. Org. Chem.* **1975**, *40*, 2263–2264.
- [9] P. F. Hudrlik, D. Peterson, *J. Am. Chem. Soc.* **1975**, *97*, 1464–1468.
- [10] D. J. Ager, *The Peterson Olefination Reaction*, in: *Organic Reactions*, Wiley, New York, **1990**, vol. 38, pp. 1–224.
- [11] G. L. Larson, C. F. de Kaifer, R. Seda, L. E. Torres, J. R. Ramirez, *J. Org. Chem.* **1984**, *49*, 3385–3386.
- [12] T. Kawashima, N. Iwama, R. Okazaki, *J. Am. Chem. Soc.* **1992**, *114*, 7598–7599.
- [13] N. S. Mill, E. E. Burns, J. Hodges, J. Gibbs, E. Esparza, J. L. Malandra, J. Koch, *J. Org. Chem.* **1998**, *63*, 3017–3022.
- [14] A. Levy, A. Rakowitz, N. S. Mills, *J. Org. Chem.* **2003**, *68*, 3990–3998.
- [15] N. S. Mills, M. A. Benish, C. Ybarra, *J. Org. Chem.* **2002**, *67*, 2003–2012.
- [16] P. U. Biedermann, J. J. Stezowski, I. Agranat, in: *Advances in Theoretically Interesting Molecules* (Ed.: R. P. Thummel), JAI Press, Stanford, CN, **1998**, vol. 4, pp. 245–322.
- [17] P. U. Biedermann, J. J. Stezowski, I. Agranat, *Eur. J. Org. Chem.* **2001**, 15–34.
- [18] N. Assadi, S. Pogodin, S. Cohen, A. Levy, I. Agranat, *Struct. Chem.* **2009**, *20*, 541–556.
- [19] D. H. R. Barton, B. J. Wills, *J. Chem. Soc. D: Chem. Commun.* **1970**, 1226–1226.
- [20] D. H. R. Barton, *Reason and Imagination: Reflections on Research*, in: *Organic Chemistry: Selected Papers of Derek H. R. Barton*, Imperial College Press and World Scientific, Singapore, **1996**, vol. 6, p. 489.
- [21] Z. Wang, *Barton–Kellogg Olefination*, in: *Comprehensive Organic Name Reactions and Reagents*, Wiley, **2009**, vol. 1, chapter 56, pp. 249–253.
- [22] H. Gilman, R. A. Benkeser, G. E. Dunn, *J. Am. Chem. Soc.* **1950**, *72*, 1689–1691.
- [23] E. D. Bergmann, *Bull. Res. Council Isr.* **1956**, *5a*, 150–154.
- [24] A. Streitwieser Jr., S. M. Brown, *J. Org. Chem.* **1988**, *53*, 904–906.
- [25] A. Levy, M. Goldschmidt, I. Agranat, *Lett. Org. Chem.* **2006**, *3*, 579–584.
- [26] *Dictionary of Organic Compounds* (Eds.: J. I. G. Cadogan, S. V. Ley, G. Pattenden, R. A. Raphael, C. W. Rees), Chapman & Hall, **1996**, vol. 1, p. 772.
- [27] M. Rabinovitz, I. Agranat, A. Weitzen-Dagan, *Tetrahedron Lett.* **1974**, *15*, 1241–1244.
- [28] N. H. Martin, N. W. Allen III, K. D. Moore, L. Vo, *THEO-CHEM* **1998**, *454*, 161–166.
- [29] Z. Wang, *Haller–Bauer Cleavage*, in: *Comprehensive Organic Name Reactions and Reagents*, Wiley, **2009**, vol. 2, chapter 291, p. 1310.
- [30] G. Mehta, R. V. Venkateswaran, *Tetrahedron* **2000**, *56*, 1399–1422.
- [31] A. Streitwieser Jr., R. G. Lawler, *J. Am. Chem. Soc.* **1963**, *85*, 2854–2855.
- [32] B. N. Papas, S. Wang, N. J. DeYonker, H. L. Woodcock, H. F. Schaefer III, *J. Phys. Chem. A* **2003**, *107*, 6311–6316.
- [33] A. G. Brook, *Acc. Chem. Res.* **1974**, *7*, 77–84.
- [34] Z. Wang, *Peterson Olefination*, in: *Comprehensive Organic Name Reactions and Reagents*, Wiley, **2009**, vol. 1, chapter 117, pp. 529–535.
- [35] F. de Proft, P. Geerlings, *Chem. Rev.* **2001**, *101*, 1451–1464.
- [36] W. Koch, M. C. Holthausen, *A Chemist's Guide to Density Functional Theory*, Wiley-VCH, Weinheim, Germany, **2000**.
- [37] P. U. Biedermann, J. J. Stezowski, I. Agranat, *Chem. Commun.* **2001**, 954–955.
- [38] S. Pogodin, I. D. Rae, I. Agranat, *Eur. J. Org. Chem.* **2006**, 5059–5068.
- [39] N. S. Mills, M. Benish, *J. Org. Chem.* **2006**, *71*, 2207–2213.
- [40] S. Pogodin, I. Agranat, *J. Org. Chem.* **2007**, *72*, 10096–10107.
- [41] T. M. Krygowski, M. K. Cyrański, *Chem. Rev.* **2001**, *101*, 1385–1419.
- [42] A. Schönberg, W. I. Awad, N. Latif, *J. Chem. Soc.* **1951**, 1368–1378.
- [43] M. J. Frisch, G. W. Trucks, H. B. Schlegel, G. E. Scuseria, M. A. Robb, J. R. Cheeseman, J. A. Montgomery Jr., T. Vreven, K. N. Kudin, J. C. Burant, J. M. Millam, S. S. Iyengar, J. Tomasi, V. Barone, B. Mennucci, M. Cossi, G. Scalmani, N. Rega, G. A. Petersson, H. Nakatsuji, M. Hada, M. Ehara, K. Toyota, R. Fukuda, J. Hasegawa, M. Ishida, T. Nakajima, Y. Honda, O. Kitao, H. Nakai, M. Klene, X. Li, J. E. Knox, H. P. Hratchian, J. B. Cross, C. Adamo, J. Jaramillo, R. Gomperts, R. E. Stratmann, O. Yazyev, A. J. Austin, R. Cammi, C. Pomelli, J. W. Ochterski, P. Y. Ayala, K. Morokuma, G. A. Voth, P. Salvador, J. J. Dannenberg, V. G. Zakrzewski, S. Dapprich, A. D. Daniels, M. C. Strain, O. Farkas, D. K. Malick, A. D. Rabuck, K. Raghavachari, J. B. Foresman, J. V. Ortiz, Q. Cui, A. G. Baboul, S. Clifford, J. Cioslowski, B. B. Stefanov, G. Liu, A. Liashenko, P. Piskorz, I. Komaromi, R. L. Martin, D. J. Fox, T. Keith, M. A. Al-Laham, C. Y. Peng, A. Nanayakkara, M. Challacombe, P. M. W. Gill, B. Johnson, W. Chen, M. W. Wong, C. Gonzalez, J. A. Pople, *Gaussian 03*, rev. C.02, Gaussian, Inc., Wallingford CT, **2004**.
- [44] A. D. Becke, *J. Chem. Phys.* **1993**, *98*, 5648–5652.
- [45] C. Lee, W. Yang, R. G. Parr, *Phys. Rev. B* **1988**, *37*, 785–789.

Received: June 2, 2011

Published Online: September 22, 2011